

Computing the viscosity of the QGP on the lattice

Harvey B. MEYER^{1,*})

¹*Center for Theoretical Physics, Massachusetts Institute of Technology
77 Massachusetts Avenue, 02139 Cambridge, USA*

I review the recent progress made in calculating shear and bulk viscosity on the lattice, and discuss ways to improve the calculation.

§1. Introduction

Models treating the system produced in heavy ion collisions at RHIC as an ideal fluid have had significant success in describing the observed large elliptic flow.^{1),2)} Subsequently the leading corrections due to a finite shear viscosity η were estimated³⁾ and led to a remarkably small upper bound on η . Recent relativistic viscous hydrodynamics simulations^{4)–6)} have started to achieve a tighter control over the systematic sources of uncertainty on the extraction of the shear viscosity to entropy density ratio, η/s . On the theory side, it is therefore important to compute the QCD shear viscosity from first principles to complete the picture. Furthermore, since the heavy ion collision program at LHC will probe the quark-gluon plasma at temperatures about a factor two higher, it is crucial to predict the shear viscosity at $\approx 3T_c$, and from there to predict the size of elliptic flow, before experimental data is available.

A small transport coefficient is a signature of strong interactions; strong interactions in turn require non-perturbative computational techniques. In this talk I present a lattice calculation of the thermal correlators of the energy-momentum tensor in the Euclidean SU(3) pure gauge theory, and discuss methods to extract the shear and bulk viscosity from them. Computationally, the calculation is challenging enough without the inclusion of dynamical quarks, and physically, the thermodynamic properties of the QGP not too close to T_c do not depend sensitively on the flavor content.⁷⁾ In perturbation theory,⁸⁾ the ratio of shear viscosity to entropy density of the pure gauge theory only differs by about 30% from full QCD⁹⁾ at a fixed value of α_s (η/s is smaller in the pure gauge theory). It should be appreciated that this is not much for a quantity which is infinite in the Stefan-Boltzmann limit, and the difference is actually reduced when comparing the pure gauge theory and full QCD at a common value of T/T_c .

Lattice calculations of the shear viscosity^{10)–12)} are based on Kubo formulas (see e.g.¹³⁾ and¹⁴⁾), which relate each transport coefficient to the small frequency behavior of the retarded correlator. By analytic continuation (see Appendix A), the latter is related to the Euclidean two-point function of the conserved current. The significant progress made in¹²⁾ was to obtain the energy-momentum correlators with an accuracy of about 3% on (isotropic) lattices with temporal resolution up to

*) E-mail: meyerh@mit.edu

$N_\tau = 12$. This progress was mainly due to the use of a multi-level algorithm.¹⁵⁾

Besides technical improvements that concern the discretization of the correlators, I present new ideas to enhance the sensitivity of the lattice data to the low-frequency region of the spectral function, which determines the transport properties. Subtracting correlators with different spatial momentum \mathbf{p} or different temperature T will cancel off most of the contribution of the high-frequency modes. The task is then to solve for the difference of the spectral functions for two different values of \mathbf{p} or T . This difference is no longer positive definite and solving for the spectral function requires new methods, such as developed in Ref.¹⁶⁾

The correlators computed on the lattice are ($L_0 = 1/T$)

$$\begin{aligned} C_s(x_0, \mathbf{p}) &= L_0^5 \int d^3\mathbf{x} e^{i\mathbf{p}\cdot\mathbf{x}} \langle T_{12}(0)T_{12}(x_0, \mathbf{x}) \rangle, \\ C_b(x_0, \mathbf{p}) &= \frac{L_0^5}{9} \sum_{i,j=1}^3 \int d^3\mathbf{x} e^{i\mathbf{p}\cdot\mathbf{x}} \langle T_{ii}(0)T_{jj}(x_0, \mathbf{x}) \rangle. \end{aligned} \quad (1.1)$$

For our purposes the spectral functions are then defined by

$$C_{s,b}(x_0, \mathbf{p}) = L_0^5 \int_0^\infty \rho_{s,b}(\omega, \mathbf{p}) \frac{\cosh \omega(\frac{1}{2}L_0 - x_0)}{\sinh \frac{\omega L_0}{2}} d\omega. \quad (1.2)$$

The shear and bulk viscosities are given by¹⁰⁾

$$\eta(T) = \pi \lim_{\omega \rightarrow 0} \frac{\rho_s(\omega, \mathbf{0})}{\omega}, \quad \zeta(T) = \pi \lim_{\omega \rightarrow 0} \frac{\rho_b(\omega, \mathbf{0})}{\omega}. \quad (1.3)$$

The spectral functions are positive, $\rho(\omega, \mathbf{p})/\omega \geq 0$, and odd, $\rho(-\omega, \mathbf{0}) = -\rho(\omega, \mathbf{0})$. If not specified, \mathbf{p} is set to zero in this talk. In Ref. 16), I defined the following moments of the spectral function ($n = 0, 1, \dots$):

$$\langle \omega^{2n} \rangle \equiv L_0^5 \int_0^\infty d\omega \frac{\omega^{2n} \rho(\omega)}{\sinh \omega L_0/2} = \left. \frac{d^{2n} C}{dx_0^{2n}} \right|_{x_0=L_0/2} \quad (1.4)$$

The latter equality implies that they are directly accessible to lattice calculations.

A first observation is that in infinite spatial volume and in the continuum limit,

$$C_s(x_0, \mathbf{p}) = \frac{L_0^5}{4} \int d^3\mathbf{x} e^{i\mathbf{p}\cdot\mathbf{x}} \langle (T_{11} - T_{22})(0)(T_{11} - T_{22})(x_0, \mathbf{x}) \rangle, \quad \mathbf{p} = (0, 0, p). \quad (1.5)$$

All the results concerning C_s presented in this talk have been obtained by discretizing this form. Secondly, because $T_{ii} = T_{\mu\mu} - T_{00}$, and because $\int d^3\mathbf{x} \langle T_{00}(x)\mathcal{O}(0) \rangle_c = T^2 \partial_T \langle \mathcal{O} \rangle_T$ for any local operator \mathcal{O} and $x_0 \neq 0$,

$$\int d^3\mathbf{x} \langle T_{\mu\mu}(x) T_{\nu\nu}(0) \rangle_c = T^2 \partial_T (\epsilon - 6P) + \int d^3\mathbf{x} \langle T_{ii}(x) T_{kk}(0) \rangle_c. \quad (1.6)$$

We have used $\langle T_{ii} \rangle_{T=0} = -3P$, $\langle T_{00} \rangle_{T=0} = \epsilon$. It is therefore convenient to study the two-point function C_θ of the trace anomaly $\theta \equiv T_{\mu\mu}$.

§2. Thermal correlators from isotropic lattices

Figures (1,2) show the $\mathbf{p} = \mathbf{0}$ scalar and tensor correlators for the range of temperatures T_c to $3.2T_c$. This data was obtained on $N_\tau = 8$ lattices with the Wilson action and the ‘bare-plaquette’ discretization¹⁷⁾ of the energy-momentum tensor, and I implemented the tree-level improvement.¹²⁾ The leading cutoff effects are thus $O(g_0^2 a^2)$.

The tensor correlator exhibits near-conformal behavior, while in the scalar case large departures from conformality are seen, particularly near T_c . The curves are the leading-order perturbative results. For the scalar correlator,¹⁶⁾ which is $O(\alpha_s^2)$, a choice has to be made for the value of the coupling. The value that matches the LO prediction for $\epsilon - 3P$ with the non-perturbative value¹⁸⁾ at $3.22T_c$ is $\alpha_s(2\pi T) = \alpha_s^* \equiv 0.289$.¹⁶⁾ I then use the one-loop evolution on Fig. (2), $\alpha_s(2\pi x_0^{-1}) = \alpha_s^*/(1 - \frac{11}{2\pi}\alpha_s^* \log(Tx_0))$. The non-perturbative correlator is somewhat flatter than the LO perturbative prediction. A study of cutoff effects¹⁶⁾ for $T_c < T < 2T_c$ shows that the $N_\tau = 8$ data at $x_0 = L_0/2$ is an overestimate, at most by 20%, of the continuum correlator. Large finite-size effects can be excluded on the basis of the large aspect ratio, $LT = 6$.

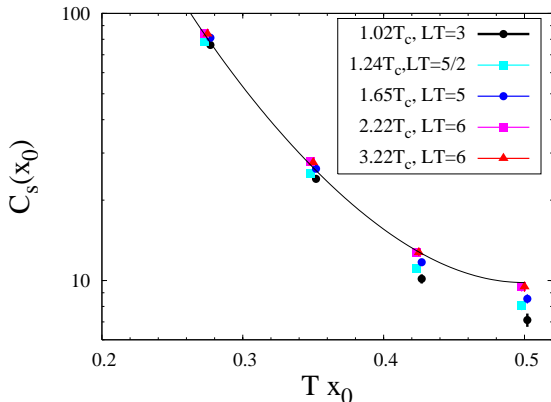


Fig. 1. The tensor correlator C_s for different temperatures

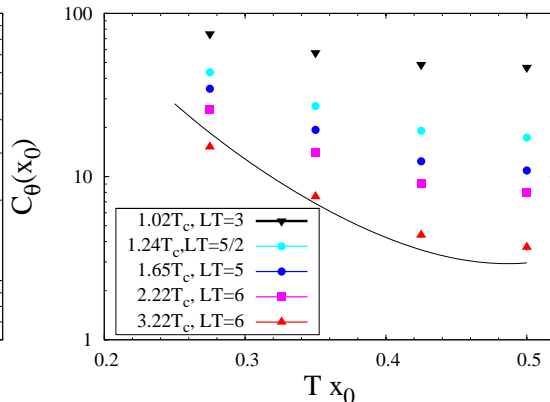


Fig. 2. The scalar correlator C_θ for different temperatures.

Figure (3) displays the first two moments, Eq. (1.4), of the tensor spectral function at $\mathbf{p} = \mathbf{0}$. They are normalized by the leading perturbative result.¹²⁾ I also show the corresponding ratio of moments in the (conformal) $\mathcal{N} = 4$ SYM theory,^{13),19)} computed by AdS/CFT methods. It is remarkable that the typical size and the sign of the deviations from the free approximation is the same in both theories.

Based on the data displayed on Fig. (1,2) and data at smaller spacing, I estimated^{12),16)} the shear and bulk viscosity by expanding the spectral function linearly in a set of orthogonal functions $u_\ell(\omega)$. In this way I obtained for instance $\eta/s = 0.13(3)$ at $1.65T_c$. Due to the small size N_p of the set, the functions fail to satisfy the completeness relation by an amount quantified by the resolution function $\hat{\delta}(\omega, \omega') = \sum_{\ell=1}^{N_p} u_\ell(\omega)u_\ell(\omega')$. Figure (4) shows the resolution function for $\omega'/T = 0$,

10 and 20 for $N_p = 4$. It is broad, and quite far from resembling a delta function at $\omega = \omega'$. Nevertheless, in cases where the spectral function is smooth, such as the strongly coupled SYM theory,^{13),19)} the method works well, see Fig. (4).

Figure (3) demonstrates that even at $1.6T_c$, the deviation of the first moment, to which the transport peak contributes, from the non-interacting approximation, is only about 10%. This observation had previously been made in the finite-temperature perturbation theory framework²⁰⁾ and in the strongly coupled SYM theory.¹³⁾ It therefore appears necessary to investigate the analytic structure of the spectral function to understand where this lack of sensitivity to the low-energy degrees of freedom comes from.

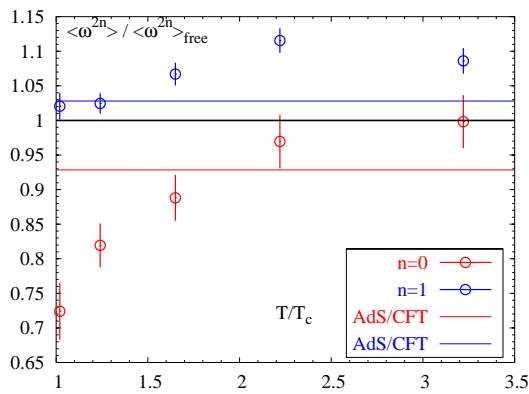


Fig. 3. The lowest two moments of the tensor spectral function for $N_\tau = 8$ on the isotropic lattice.

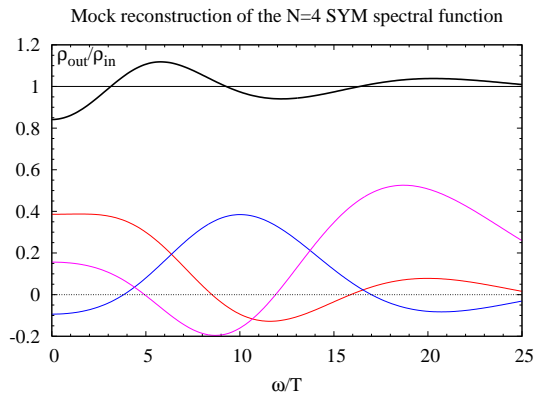


Fig. 4. Reconstruction of the SYM spectral function from the $N_\tau = 8$ Euclidean correlator; resolution functions at 3 points are shown.

§3. Analytic structure of the spectral function

The leading-order perturbative behavior of the spectral functions can be found in Ref. 12), 16), they grow as ω^4 at high frequencies, and at $T = 0$ the NLO corrections in α_s are known.^{21),22)} Furthermore, at $T = 0$, Lorentz invariance implies

$$\rho(\omega, \mathbf{p}) = \text{sgn}(\omega)\theta(\omega^2 - \mathbf{p}^2) \rho(\sqrt{\omega^2 - \mathbf{p}^2}, \mathbf{0}) \quad (3.1)$$

in the scalar channel. Based on the operator product expansion,²³⁾ we expect the perturbative series of the ω^4 coefficient to be independent of temperature. Therefore, this term, which makes a large contribution to the Euclidean correlators without telling us anything about thermal physics, can be eliminated by subtracting the $T = 0$ spectral function from the finite-temperature one.

For low momenta and frequencies, hydrodynamics predicts the functional form of the spectral functions in the shear channel and the sound channel ($\rho_{11,11}$, defined as ρ_s with T_{12} replaced by T_{11}). For $\mathbf{p} = (p, 0, 0)$, and v_s being the velocity of sound,

$$\frac{\rho_s(\omega, \mathbf{p})}{\omega} = \frac{\eta}{\pi} \frac{\omega^2}{\omega^2 + (\eta p^2 / (T s))^2}, \quad (3.2)$$

$$\frac{\rho_{11,11}(\omega, \mathbf{p})}{\omega} = \frac{\frac{4}{3}\eta + \zeta}{\pi} \frac{\omega^4}{(\omega^2 - v_s^2 p^2)^2 + (\omega p^2 (\frac{4}{3}\eta + \zeta)/(Ts))^2}. \quad (3.3)$$

See Ref. 13) for a particularly clear derivation. It is therefore of interest to study also correlators with non-vanishing spatial momentum. Ultimately, observing this structure in the spectral function is the best way to give us confidence in the extraction of the viscosities.

Finally, we remark on a subtlety in the calculation of bulk viscosity. On general grounds, ρ_b is expected to *not* have any delta function at $\omega = 0$ in an interacting theory. This would indeed reflect the conservation of (part of) the momentum current, which would imply in particular that such a current never dissipates and the system never reaches equilibrium. The spectral function for the C_θ correlator, in view of Eq. (1.6), must then contain the term $T\partial_T(\epsilon - 6P)\omega\delta(\omega)$. This singular term was missed in.¹⁶⁾

§4. Methods to enhance the sensitivity to the low-frequency region.

4.1. Strategy I: exploiting the $T = 0$ spectral function

The idea is to solve the integral equation (1.2) for the linear combination

$$\Delta\rho(T, \omega) \equiv \rho(T, \omega) - (\rho(0, \omega) - \rho_{1p}(\omega)). \quad (4.1)$$

In words, subtract the zero-temperature spectral function, except for its one-particle contributions. Indeed there are two glueballs below the two-particle threshold in both the scalar and the tensor channel. In infinite spatial volume, the function subtracted from $\rho(T, \omega)$ is exactly zero below $2M_{0++} \simeq 3\text{GeV}$. The low-frequency region is therefore unaffected, but the high-frequency asymptotics of the function to be reconstructed is now ω^0 , up to logarithms. This is a dramatic improvement.

The first step is thus to determine the $T = 0$ spectral function, on which Lorentz symmetry places much stronger constraints. The Euclidean correlators deep in the confined phase are shown on Fig. (5). They are computed with the isotropic Wilson gauge action, with $a \approx 0.068$ and 0.051 fm. The correlators fall off rapidly at large distance, where a significant signal is obtained only due to the multi-level algorithm. The correlators have been treelevel improved.^{12), 16)} After this improvement, the two-loop perturbative prediction²¹⁾ of the tensor correlator and the one-loop prediction for the scalar channel (both with α_s set to 0.25) compare rather well with the data at short distance. At large distance $x_0 > 0.5$ fm, the data is compared to the contribution from ρ_{1p} , namely that of the two stable glueballs present in each channel. I took their masses from²⁵⁾ and computed their matrix elements separately.²⁷⁾

4.2. Strategy II: linear combinations of $\mathbf{p} \neq 0$ spectral functions

From Eq. (3.1), we expect that for $\omega \gg T$, the ω^4 contribution cancels up to two-loop order in the linear combination

$$\rho(\omega, \mathbf{0}) - \frac{b}{b-1} \rho(\omega, \frac{\mathbf{p}}{\sqrt{b}}) + \frac{1}{b-1} \rho(\omega, \mathbf{p}), \quad b > 1. \quad (4.2)$$

In the tensor channel, this means that the leading large- ω behaviour of this linear combination is $O(\alpha_s^2 \omega^4)$. Figure (6) displays linear combination (4.2) of the correlators C_s for $b = 4$ and $\mathbf{p} = (0, 0, \pi T)$. A cancellation by almost two orders of magnitude takes place and the data is consistent with zero at all x_0 . This is a remarkable fact; by contrast $C_s(x_0, \mathbf{0}) - C_s(x_0, \frac{1}{2}\mathbf{p})$ does not vanish. Obviously such linear combinations deserve further investigation. The data on Fig. (6) was obtained on an anisotropic lattice with the clover discretization¹⁷⁾ of the energy-momentum tensor, with non-perturbative normalization factors determined using the thermodynamics data in Ref. 26).

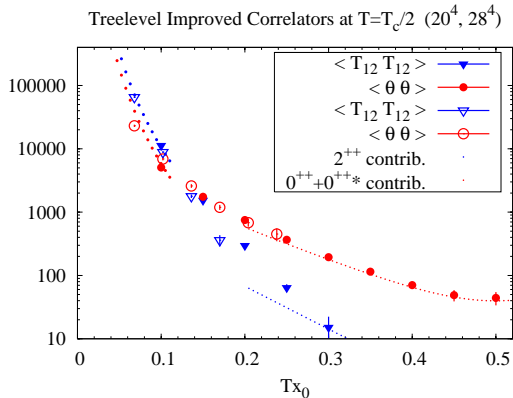


Fig. 5. C_s and C_θ in the confined phase.

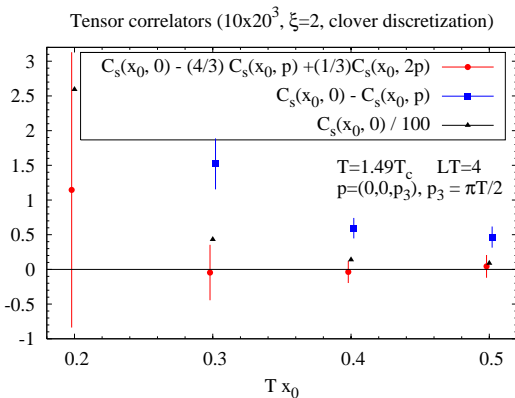


Fig. 6. Treelevel improved tensor correlators.

§5. Conclusion

The correlators of the energy-momentum tensor contain information on the plasma that is complementary to that of thermodynamics. They are sensitive to the low-energy degrees of freedom rather than the bulk of them, in particular they contain the information on the transport properties of the system.

Describing the Euclidean data with a smooth spectral function consistent with positivity, parity and the perturbative large-frequency prediction leads to a low shear viscosity to entropy ratio,¹²⁾ $1 < 4\pi\eta/s < 2$ in the temperature range $1.2 < T/T_c < 1.7$.

In order to increase the sensitivity of the Euclidean correlators to the low-frequency domain of the spectral function, I have proposed two different strategies that aim at subtracting the contributions of high-frequency modes. The goal is to challenge the smoothness assumption made on the spectral function.^{12), 16)}

A central question is whether perturbation theory can explain most properties of the plasma at $\approx 3T_c$, a typical temperature probed at LHC. If it is to account correctly for the viscosities, then it should accurately describe the corresponding Euclidean correlators. In the scalar channel at $3.2T_c$, the agreement of LO perturbation theory with the lattice data depends sensitively on the choice of coupling value. Figure (3) suggest that the agreement is good in the tensor channel at $3.2T_c$, how-

ever the data is also compatible with a strongly coupled scenario, as the qualitative comparison with AdS/CFT reveals. The methods I presented to subtract the UV-contributions have the potential to elucidate which is the more appropriate picture of the plasma at temperatures typical of the LHC experiments.

Acknowledgements

I am grateful to the organizing committee of the New Frontiers in QCD 2008 workshop, in particular to Kenji Fukushima, for the kind invitation extended to me. Of all the interesting discussions I enjoyed at the workshop, I would like to especially mention those with G. Aarts, B. Mueller, D. Teaney, R. Venugopalan that were directly relevant to this work.

Appendix A

— Analytic continuation of the retarded correlator —

Our goal in this section is to relate the spectral function of a conserved operator, defined via a Euclidean correlator, to the imaginary part of the retarded Green's function in frequency space. A Kubo formula relates the latter to a transport coefficient of the finite-temperature system, in the case of a conserved operator; for the shear viscosity, $\eta = -\lim_{\omega \rightarrow 0} \frac{1}{\omega} \text{Im} G_R^{12,12}(\omega)$, where $G_R^{12,12}$ is the retarded Green's function of T_{12} (see Ref. 13), 14).

The Euclidean correlator, $C_E(t) = \langle \mathcal{O}(t)\mathcal{O}(0) \rangle$, $t > 0$, has the spectral representation

$$C_E(x_0) = \frac{1}{Z} \sum_{n,m} |\mathcal{O}_{nm}|^2 e^{-L_0 E_n} e^{E_{nm} x_0}. \quad (\text{A}\cdot 1)$$

Here $\mathcal{O}_{nm} = \langle n | \mathcal{O} | m \rangle$, $E_{nm} = E_n - E_m$. One easily finds that $C_E(t)$ can be expressed in terms of the spectral function $\rho(L_0, \omega)$ (see Eq. 1·2)

$$\rho(L_0, \omega) = \frac{2}{Z} \sinh(\omega L_0/2) \sum_{n,m} \delta(\omega - E_{nm}) e^{-(E_n + E_m)L_0/2} |\mathcal{O}_{nm}|^2. \quad (\text{A}\cdot 2)$$

On the Minkovsky side, the retarded correlator $iG_R(t) = \theta(t) \langle [\mathcal{O}(t), \mathcal{O}(0)] \rangle$ has the spectral representation

$$iG_R(t) = \frac{\theta(t)}{Z} \sum_{n,m} |\mathcal{O}_{nm}|^2 e^{-L_0 E_n} (e^{iE_{nm}t} - e^{-iE_{nm}t}). \quad (\text{A}\cdot 3)$$

It is related to the Euclidean correlator by the relation

$$iG_R(t) = \lim_{\epsilon \rightarrow 0} (C_E(it + \epsilon) - C_E(-it + \epsilon)), \quad t > 0. \quad (\text{A}\cdot 4)$$

A small positive real part in the argument of C_E guarantees the finiteness of the expression. In terms of the spectral function, we obtain

$$iG_R(t) = \lim_{\epsilon \rightarrow 0} \int_{-\infty}^{\infty} d\omega \rho(L_0, \omega) e^{-i\omega t} e^{-|\omega|\epsilon}, \quad t > 0. \quad (\text{A}\cdot 5)$$

We have exploited the fact that ρ is odd in ω , a property manifest in Eq. (A.2). The Fourier transform of G_R , $G_R(\omega) = \int_0^\infty dt e^{i\omega t} G_R(t)$, converges if we give its argument a positive imaginary part:

$$G_R(\omega + i\delta) = - \int_{-\infty}^{\infty} d\omega' \frac{\rho(L_0, \omega') e^{-|\omega'| \epsilon}}{\omega' - \omega - i\delta}, \quad \omega \text{ real.} \quad (\text{A.6})$$

In particular,

$$\text{Im } G_R(\omega + i\delta) = \int_{-\infty}^{\infty} d\omega' (-\pi \rho(L_0, \omega') e^{-|\omega'| \epsilon}) \frac{1}{\pi} \frac{\delta}{(\omega' - \omega)^2 + \delta^2} = -\pi \rho(L_0, \omega), \quad (\text{A.7})$$

where we have recognized one of the standard representations of the delta function, and let $\epsilon \rightarrow 0$ in the last step.

References

- 1) P. F. Kolb, P. Huovinen, U. W. Heinz and H. Heiselberg, Phys. Lett. B **500**, 232 (2001); P. Huovinen, P. F. Kolb, U. W. Heinz, P. V. Ruuskanen and S. A. Voloshin, Phys. Lett. B **503**, 58 (2001).
- 2) D. Teaney, J. Lauret and E. V. Shuryak, Phys. Rev. Lett. **86**, 4783 (2001).
- 3) D. Teaney, Phys. Rev. C **68**, 034913 (2003).
- 4) P. Romatschke and U. Romatschke, Phys. Rev. Lett. **99**, 172301 (2007) [arXiv:0706.1522 [nucl-th]]; M. Luzum and P. Romatschke, arXiv:0804.4015 [nucl-th].
- 5) H. Song and U. W. Heinz, Phys. Lett. B **658**, 279 (2008) [arXiv:0709.0742 [nucl-th]]; H. Song and U. W. Heinz, arXiv:0712.3715 [nucl-th].
- 6) K. Dusling and D. Teaney, Phys. Rev. C **77**, 034905 (2008) [arXiv:0710.5932 [nucl-th]].
- 7) F. Karsch, Nucl. Phys. A **783**, 13 (2007) [arXiv:hep-ph/0610024].
- 8) P. Arnold, G.D. Moore and L.G. Yaffe, JHEP **0305**, 051 (2003).
- 9) G. D. Moore, arXiv:hep-ph/0408347.
- 10) F. Karsch and H.W. Wyld, Phys. Rev. D **35**, 2518 (1987).
- 11) A. Nakamura and S. Sakai, Phys. Rev. Lett. **94**, 072305 (2005).
- 12) H. B. Meyer, Phys. Rev. D **76**, 101701 (2007) [arXiv:0704.1801 [hep-lat]].
- 13) D. Teaney, Phys. Rev. D **74**, 045025 (2006) [arXiv:hep-ph/0602044].
- 14) D. T. Son and A. O. Starinets, Ann. Rev. Nucl. Part. Sci. **57**, 95 (2007) [arXiv:0704.0240 [hep-th]].
- 15) H.B. Meyer, JHEP **0401**, 030 (2004).
- 16) H. B. Meyer, Phys. Rev. Lett. **100**, 162001 (2008), arXiv:0710.3717 [hep-lat].
- 17) H. B. Meyer and J. W. Negele, Phys. Rev. D **77**, 037501 (2008) [arXiv:0707.3225 [hep-lat]].
- 18) G. Boyd, J. Engels, F. Karsch, E. Laermann, C. Legeland, M. Lutgemeier and B. Petersson, Nucl. Phys. B **469**, 419 (1996).
- 19) P. Kovtun and A. Starinets, Phys. Rev. Lett. **96**, 131601 (2006) [arXiv:hep-th/0602059].
- 20) G. Aarts and J.M. Martinez Resco, JHEP **0204**, 053 (2002).
- 21) A. A. Pivovarov, Phys. Atom. Nucl. **63**, 1646 (2000) [Yad. Fiz. **63N9**, 1734 (2000)] [arXiv:hep-ph/9905485].
- 22) A. L. Kataev, N. V. Krasnikov and A. A. Pivovarov, Nucl. Phys. B **198**, 508 (1982) [Erratum-ibid. B **490**, 505 (1997)] [arXiv:hep-ph/9612326].
- 23) S. Z. Huang and M. Lissia, Phys. Lett. B **348**, 571 (1995) [arXiv:hep-ph/9404275].
- 24) Y. Namekawa *et al.* [CP-PACS Collaboration], Phys. Rev. D **64**, 074507 (2001) [arXiv:hep-lat/0105012].
- 25) H. B. Meyer, Ph. D. thesis, arXiv:hep-lat/0508002.
- 26) Y. Namekawa *et al.* [CP-PACS Collaboration], Phys. Rev. D **64**, 074507 (2001) [arXiv:hep-lat/0105012].
- 27) H.B. Meyer, in preparation.